Presented at 1980 Nuclear
Science Symposium, Orlando,
Florida, 5-7 November 1980.

BNL 28691

SIGNAL SHAPING AND TAIL CANCELLATION FOR GAS PROPORTIONAL DETECTORS AT HIGH COUNTING RATES*

R. A. Boie, A. T. Hrisoho,† and P. Rehak

Brookhaven National Laboratory
Upton, New York 11973

November, 1980

*This research was supported by the U. S. Department of Energy: Contract No. DE-AC02-76CH00016.

†Present address: Laboratoire de L'Accélérateur Linéaire, Orsay, France.

SIGNAL SHAPING AND TAIL CANCELLATION FOR GAS PROPORTIONAL DETECTORS AT HIGH COUNTING RATES*

R. A. Boie, A. T. Hrisoho,† and P. Rehak

Brookhaven National Laboratory
Upton, New York 11973

Abstract

A low noise, wide bandwidth preamplifier and signal processing filter were developed for high counting rate proportional counters. The filter consists of an eight pole Gaussian integrator with symmetrical weighting function and continuously variable shaping time, τ_s, of 8 ns to 50 ns (FWHM) preceded by a second order pole/zero circuit which cancels the long (1/t) tails of the chamber signals. The preamplifier is an optimized common base input design with 2 nsec rise time and an equivalent noise input charge of < 2000 rms electrons, when connected to a chamber with 10 pF capacitance and at a filtering time, τ_s, of 10 ns.

Introduction

The signal processing filter described here realizes, by use of a low noise preamplifier, a shortening filter and a semi-Gaussian integrator, high counting rate performance for gas proportional detectors at minimum signal charge or avalanche size. The ability to operate at modest avalanche gain enhances the high rate performance by reducing space charge effects, plus all the usual advantages of ease of operation and long chamber life.

The operation of a detector at high counting rates presumes an ability to resolve or recognize signals which are closely spaced in time. The resolving time of a proportional chamber is limited by several factors. The avalanche is extended in time by the diffuse ionization cluster producing it and by other mechanisms of the avalanche formation process. The signal current we measure is a result of the motion of the ions produced in the avalanche as they drift in the electric field of the chamber. Approximate current and charge waveforms for a point ionization entering the avalanche region of a cylindrical geometry chamber[6] are illustrated in Fig. 1. The important features of the charge waveform for high counting rate applications are that a substantial fraction of the signal charge is collected in a short time, a few t_o, and that the signal current continues for a long time (typically hundreds of μsec). The characteristic chamber time constant, t_o, is of the order of 1 ns. The first fact provides the basis for high rate counting, i.e., that sufficient signal charge relative to the electronic noise is collected in a short time. The long "tail" of the signal, however, tends to obscure the measurement of any following signals.

It is most convenient, (in terms of the high rate measurement system which follows) to arrange the weighting function of the signal processing filter so that short duration unipolar signals result from the chamber signals. The filter is optimized for high rate application when the signal time width at the base line is minimized for a given signal charge and electronic noise. The filter described here has bipolar weighting with leading lobe response of a continuously adjustable semi-Gaussian integrator and a second negative lobe realized by a second order pole/zero shortening filter. The shaping time of the first lobe is related to the time extent of the avalanche formation in the chamber and the electronic noise. The second lobe shaping constants are related only to the characteristic time of the chamber, t_o. This response is realized by a cascaded second order pole/zero shortening filter and a high speed semi-Gaussian integrator.

The signal processing circuits described here were first applied to the time expansion chamber[1] measurements of relativistic rise by cluster counting,[2] and more recently by fine sampling[3] techniques. There is also a growing interest in high rate position sensitive detectors for dynamical studies in the biological sciences[4] and as a diagnostic tool for the development of fusion machines.[5]

Shortening Filter

The signal arising from a point ionization entering the avalanche region of the proportional counter is approximated by the relationship,[6]

$$i_c(t) = \frac{Q_m}{2t_o \ln(b/a)} \quad \frac{1}{(1+t/t_o)} \quad , \qquad (1)$$

where $i_c(t)$ is the chamber current, Q_m is the total charge produced in the avalanche, a and b are the anode and cathode radii, t_o is given by $[a^2 \ln(b/a)]/2\,\mu_p V_o$, where μ_p is the positive ion mobility and V_o the anode to cathode voltage and is illustrated in Fig. 1.

Relation (1) provides a useful model of observed chamber signals, except during the initial rise of the current. An abrupt rise is not physically possible and is limited here by the velocity saturation of the positive ion mobility and other broadening terms, such as the time extent of the avalanche due to diffusion of the primary ionization cluster.

From the point of view of filtering, it is useful to view the chamber current signals as the response of a linear network with impulse response,

$$h(t) = \frac{1}{(1 + t/t_o)} \quad , \qquad (2)$$

to an input signal current, $i_s(t)$, with a resulting output current,

$$i_c(t) = i_s(t) * h(t) \quad , \qquad (3)$$

where * is the symbol for convolution and $i_s(t)$ is the convolution of all broadening terms with the avalanche signal, $Q_m/2t_o \ln(b/a)$.

The output of the preamplifier, assuming negligible broadening due to its response, is

$$V_p(t) = R_p[i_s(t)*h(t)] \quad , \qquad (4)$$

*This research was supported by the U. S. Department of Energy: Contract No. DE-AC02-76CH00016.

†Present address: Laboratoire de L'Accélérateur Linéaire, Orsay, France.

where R_p is the "transresistance" of the preamplifier.

The signal $R_p \cdot i_s(t)$ can, in principle, be recovered by passing the preamplifier signal through a linear network with response f(t) which is the inverse of h(t), i.e., $f(t)*h(t) = 1$. The response f(t) can, for practical purposes, be realized by two cascaded pole/zero networks.

The function h(t) must be decomposed into a mathematically tractable form if the filter with response f(t), which when convolved with h(t) gives a suitably shortened response s(t), is to be found. For example, a decomposition into a sum of three exponential functions provides a good approximation of h(t) and is a desirable form for finding f(t).

$$h(t) \approx e(t) = A \exp(-t/\alpha t_o) + B \exp(-t/\beta t_o) + C \exp(-t/\gamma t_o)^* \quad (5)$$

The suitability of the approximation obtained for the listed values for A,B,C,α,β, and γ is illustrated in Fig. 2 where h(t)-e(t) is plotted.

Pole/Zero Shortening Filters

A pole/zero network is shown in Fig. 3. The transfer function of this network in the Laplace domain is given by,

$$f_1(p) = \frac{P + \frac{1}{T}}{P + \frac{k}{T}} \quad , \quad (6)$$

where $T = R_1 C_1$ and $k = \frac{R_1+R_2}{R_2}$.

The response of this network to the signal e(p) is

$$V_{f_1}(p) = f_1(p) \cdot e(p) = \left(\frac{P+\frac{1}{T}}{P+\frac{k}{T}} \right) \left(\frac{A}{P+\frac{1}{\alpha t_o}} + \frac{B}{B+\frac{1}{\beta t_o}} + \frac{C}{P+\frac{1}{\gamma t_o}} \right) . \quad (7)$$

The time constant, T, is adjusted for $T = \beta t_o$, cancelling the pole at $-1/\beta t_o$. The constant k is adjusted so that all terms containing time constant T/k add to zero. The cancellation of all terms in T/k by adjustment of k is not a general property of the network but relies on the fact that $\gamma \gg \beta \gg \alpha$. The network response to the sum of these three exponential signals contains only terms with time constants αt_o and γt_o. Similarly, a second pole/zero network, with response $f_2(t)$, can be added with constants adjusted so that the only remaining terms contain time constant αt_o.

The response of the first pole/zero network to the signal e(t) is

$$V_{f_1}(t) = .99 \exp(-t/\alpha t_o) + .01 \exp(-t/\gamma t_o) \quad , \quad (8)$$

where $T = \beta t_o$ and $k = 2.5$, and the output of the second pole/zero network is

$$V_{f_2}(t) = \exp(-t/\alpha t_o) \quad , \quad (9)$$

where $T = \gamma t_o$ and $k = 1.6$.

Connecting together the chamber, preamplifier, networks f_1 and f_2, the output signal is

$$V_{f_2}(t) \propto i_s(t)*h(t)*f_1(t)*f_1(t) \approx i_s(t)*\exp(-t/\alpha t_o) \quad . \quad (10)$$

The calculated response of the chamber with response $h(t) = 1/(1+t/t_o)$, chamber plus first shortening network and chamber plus two shortening networks to a signal $i_s(t) = (Q/t_o^2)\, t \exp(t/t_o)$ is illustrated in Figs. 4(a), (b), and (c), respectively.

High Speed Semi-Gaussian Shaping Amplifier

The semi-Gaussian response is achieved by the well known technique of cascading adjustable time constant integrators. Eight integrators are used here to provide a nearly symmetrical response. The shaping times of interest for high rate proportional detector signals require time constants as low as 1 nsec for each integrator.

The coupled adjustment of eight time constants presents a formidable engineering and construction problem if conventional common shaft switching or trimming methods are used with circuits of this speed. The semi-Gaussian response is realized in an eight pole cascaded integrator with fixed capacitors and active resistors (bipolar transistors). The resistor values and thereby the time constant of each integration stage are controlled by an adjustable bias current common to all. Figure 5 illustrates the basic integration stage. The small signal impedance seen looking into the emitter of the common base transistor Q_1 is to first order resistive and with r_e given by $25\ mv/i_{Bias}$.

The transfer function of this circuit, assuming a purely resistive input impedance,

$$\frac{i_{out}(P)}{i_{in}(P)} = \frac{1}{T} \cdot \frac{1}{P+1/T} \quad , \quad (11)$$

describes an integrator with time constant $T = Cr_e$ where r_e is a linear function of the bias current. The method of cascading integrators is illustrated in the figure. The output signal and bias currents of the first transistor are the inputs for the second stage and so on.

An analysis of a common base integrator circuit, which includes its parasitic elements, reveals that for stability considerations the emitter resistance must be kept large compared to the base spreading resistance. This being the case, the description of the circuit must be modified only to include the contribution of the diffusion plus junction capacitances in the capacitor, C.

Figure 6 illustrates the schematic diagram of the shaping amplifier. The first signal shortening filter is included at its input. The second shortening filter is approximated by the base line restorer of the output amplifier. The cascaded integrator is formed by transistors Q_3-Q_{10}. The bias current is controlled by the potentiometer in Q_3 emitter circuit. The transconductance amplifier, Q_1,Q_2, provide the input signal current for the integrator. The output current of the final integration stage is converted to a voltage in the common

*A=.79; α=1.6; B=.185; β=13.5; C=.024; γ=113.

base amplifier formed by transistors Q_{11}-Q_{13}. Transistors Q_{14}-Q_{18} form a high speed voltage amplifier[7] with a wraparound base line restorer (A_1 and Q_{19}).

The integrator signal currents are nominally arranged to be small compared to the bias current. The response of the circuit is basically nonlinear since the instantaneous shaping time is inversely proportional to the signal plus bias currents. Large signals of the same sense as the bias current are processed with shorter shaping times than small signals. This may be an advantage for high rate counting applications in terms of overload recovery, since all signals tend to have the same time width at the baseline. The response nonlinearity may not, however, be generally desirable and may lead to difficulties in timing applications.

Common Base Preamplifier

A silicon bipolar transistor has superior noise performance because of their higher available gain bandwidth product than available JFET silicon transistors when used as the preamplifier input element for high rate proportional detectors. Although the JFET-transistors have very low parallel noise compared to bipolar devices and are thereby used to advantage at long shaping times for Si and Ge detectors, the shaping times of interest here are very short placing more importance on the contributions of the "series" noise sources.

A common base input preamplifier circuit can be shown to have the same noise performance as common emitter configurations with the advantage of achieving well defined gain and low input impedance without feedback connection. This is an advantage for a high bandwidth design in terms of the effect on the preamplifier's stability of the detailed nature of the chamber impedance and its connections to the preamplifier.

The noise contributions of the input transistor of a common base amplifier was described by Alberi et al.[8] The results of a detailed analysis to be presented elsewhere,[9] which includes the contributions of second stage noise, is used here in illustrating the optimization of the preamplifier design.

Figure 7 shows the schematic diagram of the preamplifier. The input transistor, Q_1, along with the follower circuits Q_2 and Q_3, comprise the preamplifier. The preamp output is connected to a second stage common base amplifier, Q_4, through a pole/zero network. For noise considerations, the collector and emitter load resistor of Q_1 must be large. The pole/zero network replaces the pole defined by the relatively long time constant of the large resistor and the capacitance at the collector of Q_1 ($\sim$ 20 ns) with a pole which has a shorter time constant. The circuit, when properly terminated, has a transresistance of 19 kΩ. The noise performance of a preamplifier-detector combination is illustrated by an expression of the noise sources in terms of the equivalent noise charge at the preamplifier input. The contributions of independent series and parallel noise sources is expressed as an equivalent noise charge, ENC_{tot}, at the preamp input by

$$\overline{ENC_{tot}^2} = \overline{ENC_p^2} + \overline{ENC_s^2} \quad , \tag{12}$$

where ENC_p and ENC_s are the parallel and series contributions.

$$\overline{ENC_p^2} = \frac{1}{2}\left[2q_o(I_{b1}+I_{b2}) + 4kT\left(\frac{1}{R_i}+\frac{1}{R_L}\right)\right]\int W(t)^2dt \tag{13}$$

$$\overline{ENC^2} = \frac{1}{2}\left[\tau_o^2\left(\frac{4kT}{r_{e1}} + 2q_oI_{b2}\right)\right]\int W'(t)^2dt \tag{14}$$

where q_o is the charge of the electron, I_{b1} and I_{b2} the first and second stage transistor base leakage currents, k is Boltzmann's constant, T the absolute temperature, R_i and R_L are the emitter and collector load resistors for the first stage, W(t) is the weighting function of the filter. The emitter resistance of the first stage is r_{e1}, where $r_{e1} = 1/gm$ the transistor transconductance. τ_o is given by the product $r_{e1} \times C_{IN}$ where C_{IN} is the total capacitance at the input.

The relationship for the parallel noise illustrates the importance of selecting high beta transistors, thereby minimizing the leakage currents and of arranging for large value collector and emitter load resistors for the input element. The importance of a high gain bandwidth transistor in minimizing the series noise contribution is evident in noting the contribution of the transistor diffusion capacitance, C_i, to the total input capacitance. The diffusion capacitance is easily shown to be given by the charge present in the transistor base which is proportional to the emitter current-base transit time product. The base transit time is what limits the bandwidth of the device. The higher the gain bandwidth product (the bandwidth measurement most often provided by the transistor manufacturer), at the emitter current of interest, the better the performance. The input transistor emitter current can be optimized with respect to the detector capacitance. In the optimal condition the device diffusion capacitance equals the capacitance of the detector. Assuming large value resistors for R_L and R_i, and a high beta for transistor Q_2, a minimum in the noise is found with respect to I_{e1} by

$$I_{e1} = \frac{kT}{q_o}\frac{C_{IN}}{t_m}\sqrt{\frac{2a_{F1}}{a_{F2}}\,h_{fe}(Q_1)} \tag{15}$$

where $a_{F1} = t_m\int W'(t)^2dt$ (16)

$$a_{F2} = \frac{1}{t_m}\int W(t)^2dt \tag{17}$$

and t_m is the time width measure of the weighting function.

Results

The impulse response of the Gaussian filter-shortening filter combination is illustrated in Fig. 8. The shortening filter constants are set quite long here to better illustrate the highly symmetrical first lobe of the Gaussian integrator and the second lobe of the shortening filter. Figure 9 illustrates the paired pulse impulse response of the filter, with shortening filter removed, as compared to that of an ORTEC 474 Timing Filter Amplifier. The time constants of each filter were adjusted for equal detector system signal-to-noise performance. The advantage of the symmetrical response filter for high rate counting is clearly evident.

The response of the preamplifier to an impulse of charge (1×10^5 electrons) is shown in Fig. 10. The measured output signal shape corresponds to that of two cascaded integrators with $\sim$ 1 ns time constant which is consistent with the minimum shaping time requirements of the following filters. The measured input equivalent noise charge for the preamplifier with transistors and operating currents illustrated in Fig. 7 for a unipolar Gaussian weighting (FWHM = 10 ns) and an added input

capacitance of 10 pF is ~ 1700 electrons. The measurement is in reasonable agreement with the value calculated using relationships (13) and (14) (1300 electrons). Figures 11(a) and 11(b) illustrate the response of a detector system to Cu K x-rays. The gas proportional chamber is Xe-filled at one atmosphere. Figure 11(a) shows the response of the system without shortening filter to an electrical impulse of charge injected into the preamplifier input (bright trace) and that due to the x-rays. Figure 11(b) shows the improved response obtained by including the shortening filter. The bright trace again is due to injected electrical signal and illustrates the bipolar weighting of the filter and the shortening of the chamber signals achieved. The signal charge from the chamber was, in each case, 10^6 electrons (integrated over 1 μsec).

Acknowledgements

We gratefully acknowledge the many fruitful technical discussions with J. Alberi, E. Gatti, and V. Radeka. F. Densing and D. Stephani are acknowledged for their technical expertise in the layout and construction of the circuits described here.

References

1. A. H. Walenta, IEEE Trans. Nuc. Sci. NS-26, No. 1, Feb. (1979) 73-80.

2. P. Rehak and A. H. Walenta, IEEE Trans. Nuc. Sci. NS-27, No. 1, Feb. (1980) 54-58.

3. T. Ludlum and E. Platner, Relativistic Rise Measurements with Very Fine Sampling Intervals, (submitted to these Proceedings).

4. J. Stamatoff, T. Bilash, V. Ching, and P. Eisenberger, Bio. Phys. J. Vol. 28 (1979) 413-422.

5. K. Hill et al., Bull. Am. Phys. Soc., Vol. 25, Oct. (1980) 998.

6. V. Radeka, IEEE Trans. Nuc. Sci. NS-21, No. 1, Feb. (1974) 51.

7. H. Spieler, IEEE Trans. Nuc. Sci. NS-27, No. 1, Feb. (1980) 302-307.

8. J. L. Alberi and V. Radeka, IEEE Trans. Nuc. Sci. NS-23, No. 1, Feb. (1976) 251-258.

9. A. Hrisoho, (to be published).

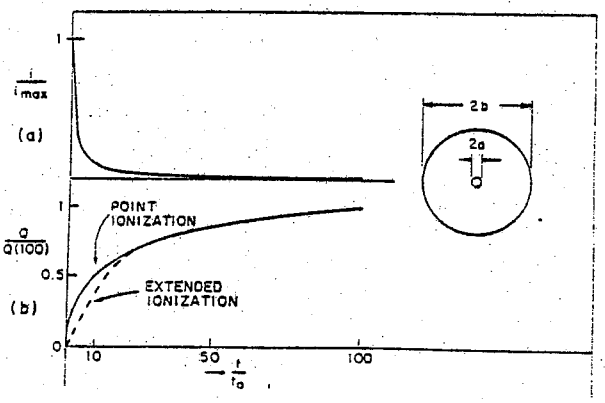

Fig. 1. Calculated output current and charge for a cylindrical geometry proportional counter for a point ionization as described in relation (1).

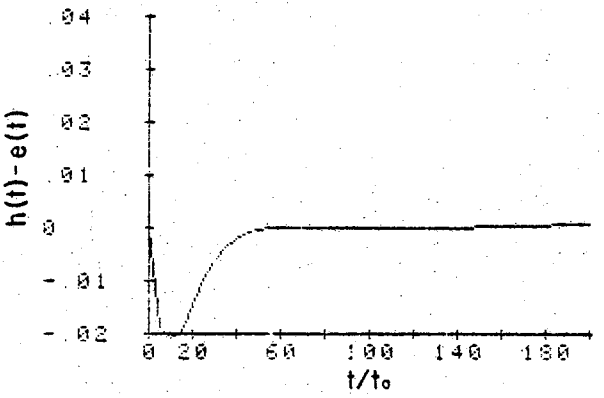

Fig. 2. Calculated difference between the function $h(t)=1/(1+t/t_o)$ and the sum of three exponential decomposition, e(t).

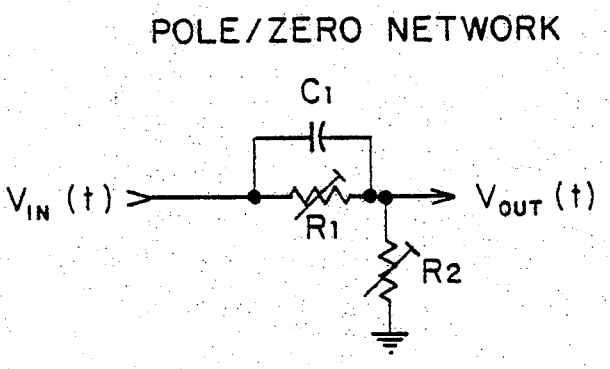

Fig. 3. Pole/zero network with response $f(P) = \frac{P + \frac{1}{T}}{P + \frac{k}{T}}$ where $T = C_1R_1$, $k = (R_1+R_2)/R_2$.

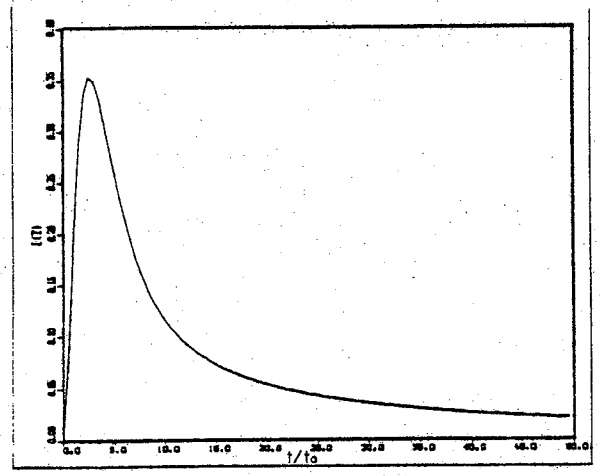

Fig. 4(a) Calculated response of the chamber output convolued with two integrations of time constant equal to, t_o.

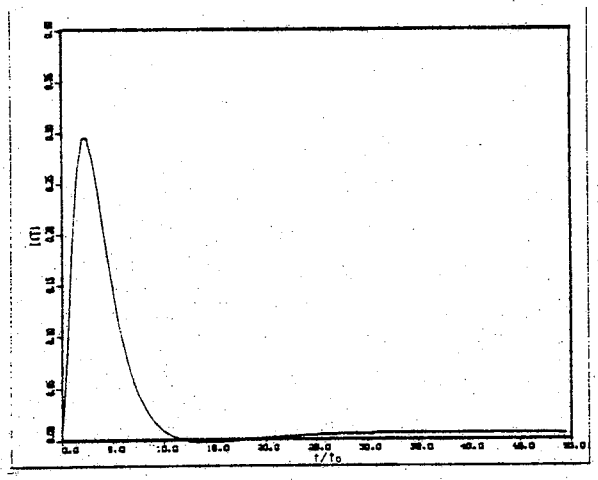

Fig. 4(b) Output response of the first pole/zero network to the signal of Fig. 4(a).

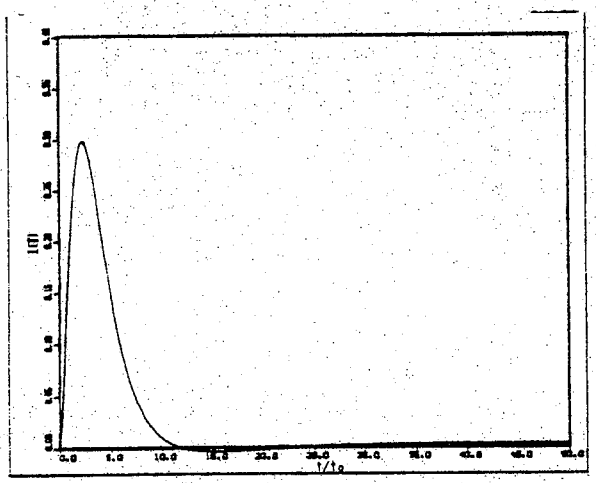

Fig. 4(c) Output response of the second pole/zero network to the signal of Fig. 4(b).

SEMI-GAUSSIAN INTEGRATOR

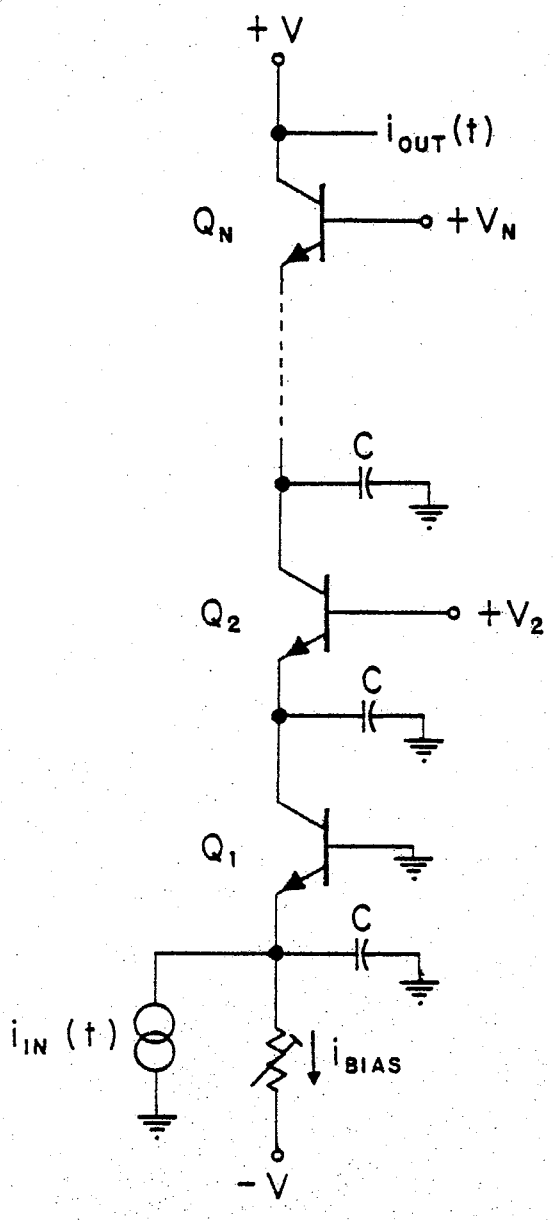

Fig. 5. Illustration of cascaded integrators formed by common base transistors operating with common bias current controlled resistors and fixed capacitors.

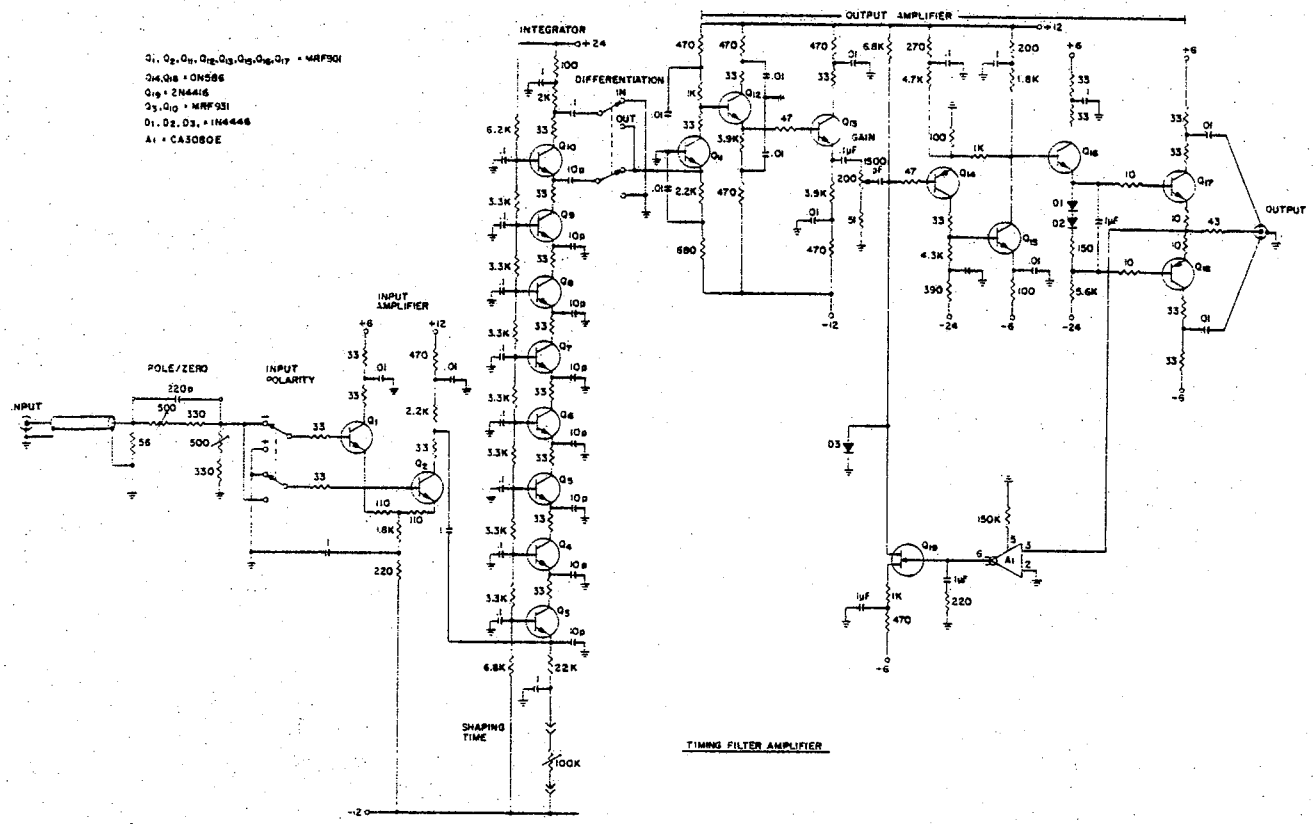

Fig. 6. Schematic diagram of the high speed semi-Gaussian integrator with shortening filter.

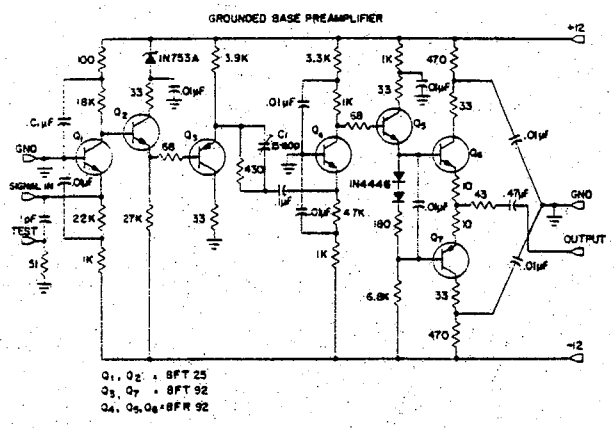

Fig. 7. Schematic diagram of the preamplifier.

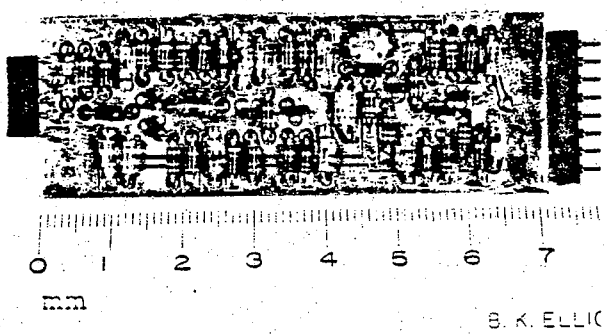

Fig. 8. Photograph of the preamplifier illustrating the construction using SOT-23 transistors. Input, test and power connections at the right end, output connection at left end of board.

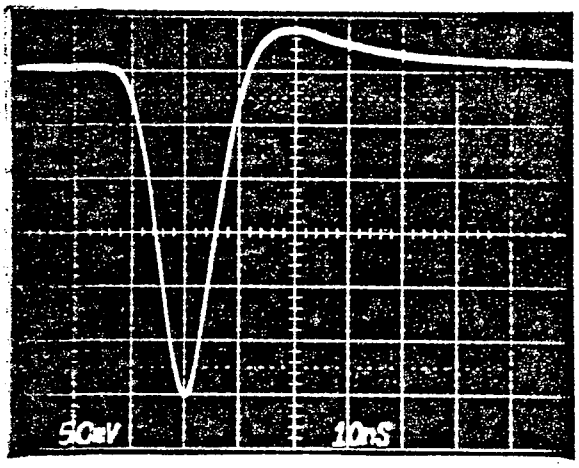

Fig. 9. Impulse response of the semi-Gaussian shortening filter.

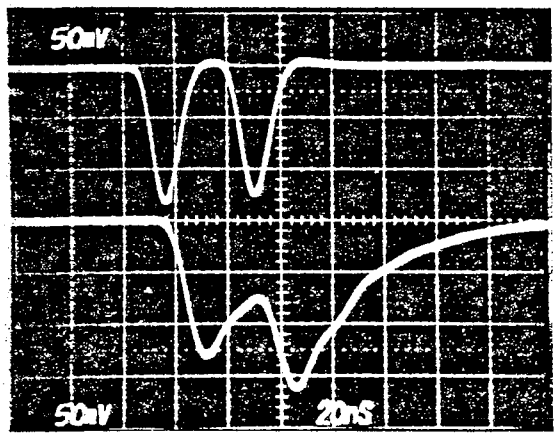

Fig. 10. Comparison of the impulse response of the semi-Gaussian filter amplifier and ORTEC 474 amplifier illustrating the advantage of the symmetrical response for high rate counting and multiple signal recognition.

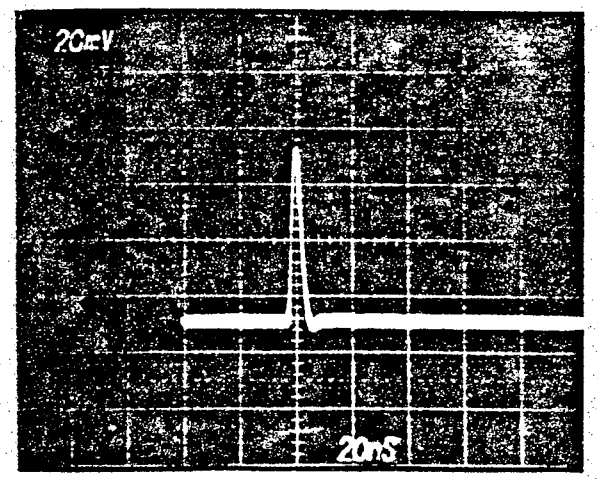

Fig. 11. Preamplifier response to a 10^5 electron impulse of charge.

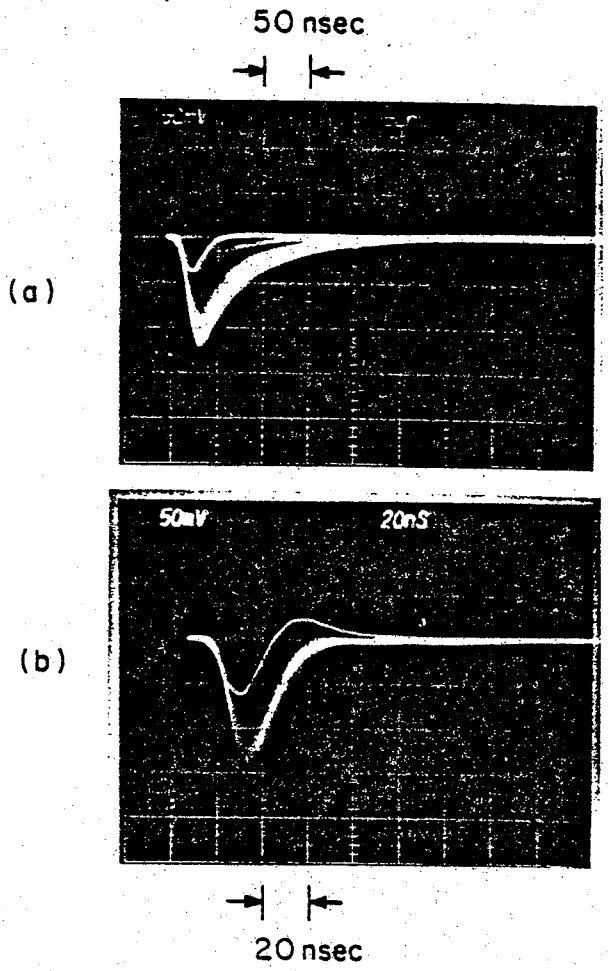

Fig. 12(a) Response of a Xe-filled chamber-preamplifier-Gaussian integrator to Cu K x-rays and to a impulse of charge injected at the pre-amplifier input (bright trace).

Fig. 12(b) Response of system with shortening filter added. Note the unipolar response to chamber signals and the bipolar response to injected charge.